Two-dimensional spatial imaging of the multiple-pulse-driven 196-Å neonlike germanium x-ray laser

Joseph Nilsen, Juan C. Moreno, Luiz B. Da Silva, and Troy W. Barbee, Jr.
Lawrence Livermore National Laboratory, Livermore, California 94550
(Received 21 August 1996)

We present two-dimensional, high-resolution, spatial images of the 196-Å laser emission from the output aperture of a neonlike germanium laser which is created by illuminating a slab target with a series of short 100-ps pulses from the Nova laser. Simulations of the gain which are propagated through the plasma density gradients to calculate the spatial distribution of the laser intensity are compared with the experiments and show good agreement. The importance of refraction in the propagation calculation manifests itself in the laser intensity peaking 150 μm from the target surface, even though the gain peaks 50 to 60 μm from the target surface. [S1050-2947(97)01101-3]

PACS number(s): 42.55.Vc, 42.60.By, 42.60.Jf

Over the last several years the neonlike $3p\ ^1S_0 \rightarrow 3s\ ^1P_1$ laser line has dominated the laser output, both in prepulse [1–6] and multiple-pulse-driven plasmas [7–9], as was originally predicted 20 years ago [10]. In this paper we use a multiple pulse technique to illuminate slab targets of germanium and measure the two-dimensional (2D) spatial distribution of the 196-Å laser intensity at the output aperture of the laser. The laser output pattern is important for understanding the mode structure and coherence of the laser and for comparing with our code predictions. These measurements also provide important data concerning the two-dimensional nature of the plasma and help to understand the nonuniformities and nonlinear effects that are important. In the past, other experiments have measured the far field angular distribution [11], which provides additional complementary information about the laser.

Experiments were conducted at Lawrence Livermore National Laboratory (LLNL) on the Nova laser using $\lambda = 0.53$ μm. One beam of the Nova laser illuminated the germanium-coated (1-μm thick) side of a 125-μm-thick, 3.0-cm-long titanium slab which had a 0.48-cm gap in the middle resulting in an actual length of 2.52 cm. The Nova laser produced a series of 100-ps full width at half maximum (FWHM) Gaussian pulses which were 400 ps apart (peak to peak). Each pulse produced 400 J of energy in a 120-μm wide (FWHM) by 3.6 cm long line focus, resulting in a peak intensity of 110 TW/cm^2. The traveling-wave setup [7] was used so that the Nova beam would illuminate the target from end to end at a phase velocity equal to the speed of light. The germanium target had a 25-μm diameter aluminum wire centered 242 μm above the target surface several hundred micrometers from the output end of the laser to serve as an absolute spatial fiducial in the measurements.

The imaging diagnostic consisted of a 50-cm radius of curvature molybdenum-silicon multilayer mirror placed 25.9 cm from the output end of the germanium laser. The multilayer mirror consisted of 20-layer pairs with a spacing of 103 Å, which gave the mirror a peak reflectivity of approximately 40% and bandwidth of 15 Å for 196-Å radiation at normal incidence. This mirror imaged the laser output on to an x-ray charge-coupled device (CCD) camera which was placed 720 cm from the mirror. A second flat molybdenum-silicon multilayer mirror was used between the imaging mirror and CCD to relay the image and block additional background. Aluminum and titanium filters were used to attenuate the signal and further eliminate shorter- and longer-wavelength signals that could be reflected off the mirrors. The CCD consisted of a 1024 by 1024 array of 24-μm pixels. The magnification used was 27.8, resulting in spatial resolution of better than 1 μm. The data were time integrated but previous experiments [7] showed that the 196-Å laser line lasted approximately 50 ps and completely dominated the spectral output. A simpler, lower magnification version of this 2D imaging diagnostic is described in Ref. [12].

We did a series of experiments using two or three pulses from the Nova laser. Experiments show that lasing occurs during the second and third Nova pulse and that the lasing during the third pulse is stronger by an order of magnitude. Figure 1 shows two-dimensional spatial images from the Nova experiments using two and three pulses. The experiment with two pulses used an order of magnitude less filtering in order to observe comparable signals on the CCD. For the case of two pulses, the lasing occurs closer to the surface (140 vs 160 μm) and has a smaller transverse extent, both in the expansion direction perpendicular to the target surface and the line focus direction parallel with the target surface, than for the case of three pulses. While the three-pulse case is time integrated over the three pulses, the third pulse completely dominates the data. For the three-pulse case, there is much structure in the laser pattern and the transverse extent of the lasing region is about 300 μm, which is twice the size for the two-pulse case and more than twice the transverse line focal width of the Nova laser. Understanding and eliminating this structure is important for improving the spatial coherence of the laser.

As suggested in our previous work [8], we believe the multiple pulses are creating a larger, more uniform density plasma, at the densities required for lasing at these short wavelengths. The first pulse heats and expands the plasma. At this time the gradients in the electron density are too steep for any significant laser propagation and the gain region is very small. However, during the second and third pulse a much larger and more uniform plasma is created, which can directly absorb the optical drive pulse and which is at the

1050-2947/97/55(1)/827(4)/$10.00

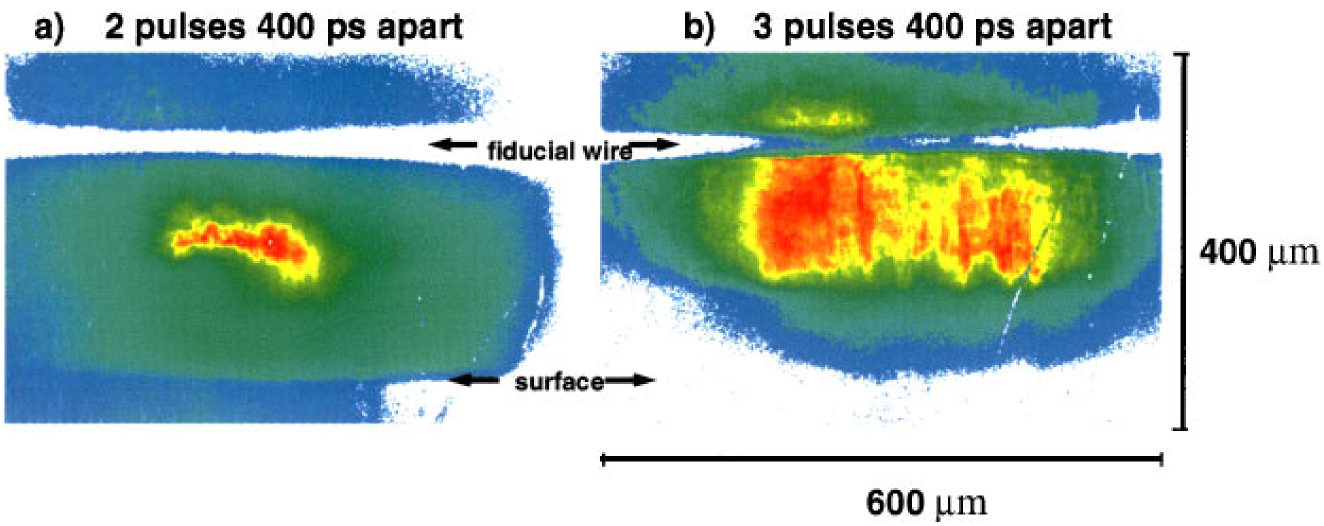

FIG. 1. (Color) Spatial image of the 196-Å laser emission at the output aperture of the germanium laser. The slab targets were illuminated by the Nova laser with either two (a) or three (b) 100-ps pulses which were 400 ps apart. The plasma expansion direction is upwards in the figure with the fiducial wire 242 μm above the target surface. The horizontal axis is in the transverse line focus direction.

right densities for gain and laser propagation. To model these experiments we did LASNEX one-dimensional computer simulations [13] of the germanium slab illuminated by three 100-ps pulses. The LASNEX calculations included an expansion angle of 15° in the dimension perpendicular to the primary expansion in order to simulate 2D effects. We also did 2D calculations to verify that this approach was valid and saw very good agreement. Using the LASNEX-calculated densities and temperatures as input to the XRASER code [14], the gains of the laser lines were calculated including radiation trapping effects on the $3s \rightarrow 2p$ transitions in neonlike germanium. Bulk Doppler effects due to the expansion of the plasmas were also included. Figure 2 shows the spatial and temporal evolution of the gain for the 196-Å line. The gain region is very small and short lived during the first Nova pulse, which peaks at 0.15 ns on this scale. During the second and third pulses, which peak at 0.55 and 0.95 ns, the gain region becomes much larger and moves further from the surface. The peak of the gain occurs 20–30 ps before the peak of the drive pulse about 50 to 60 μm from the target surface. Figure 3 shows the log of the electron density versus space and time. The electron density is truncated above the critical density of 4×10^{21} cm^{-3} to better show the position of the critical density surface. It is also truncated below 10^{19} cm^{-3} to highlight the hydrodynamics during the first pulse. During the first pulse, the density falls off exponentially and is within 50 μm of the target surface. During the second pulse the density falls off exponentially near the target sur-

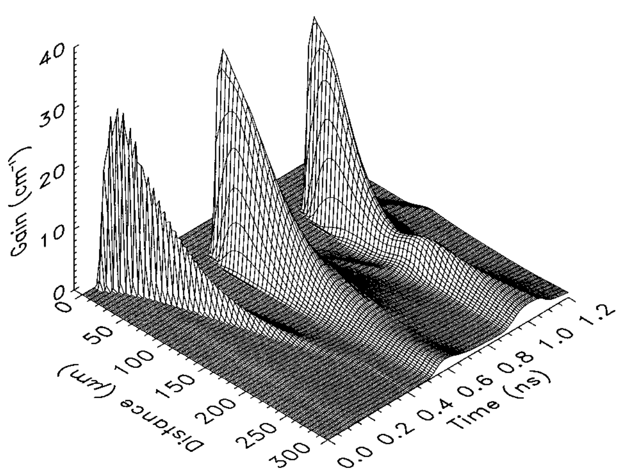

FIG. 2. Spatial and temporal evolution of the gain for the neonlike germanium 196-Å line as calculated by the XRASER code using the hydrodynamic simulations from LASNEX as input for the case of multiple-pulse illumination.

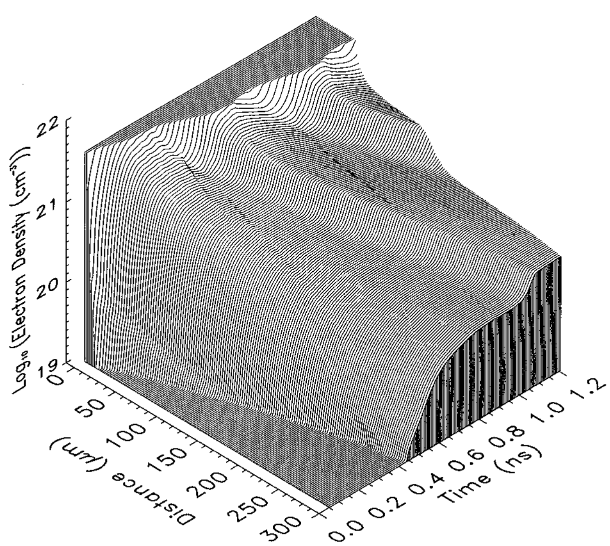

FIG. 3. The log of the electron density vs space and time for the case of multiple-pulse illumination. The data are truncated for electron densities below 10^{19} cm^{-3} and above the critical density of 4.0×10^{21} cm^{-3}.

face but then has a region of more gradual decrease starting about 60 μm from the surface. It is in the density range between 10^{20} and 10^{21} electrons per cm^3 that the gain exists. During the third pulse the gradients in the electron density becomes even smaller while the density itself increases in the region of peak gain.

The experiments show the laser emission to peak further from the surface than the calculated gain. To understand this effect, we took the gain and density profiles at the time of peak gain for the second and third Nova pulses and did propagation calculations which amplified and refracted the beam down the 2.52-cm length of the plasma. We used the population of the upper laser state as the distributed source to mock up the amplified spontaneous emission nature of these lasers. The calculation is done in the small signal regime where the effect of saturation on the gain and upper laser state populations is not included. For simplicity we neglect the effect of the gap in the target. The calculations for the second and third pulses were summed to compare with the experimental data; however, the results are completely dominated by the lasing on the third pulse. Also, with the high gain in these calculations, using a uniform source at one end of the laser gives similar results to using the distributed source discussed above. Figure 4 shows the intensity versus distance from the target surface from the refraction calculation. The figure also shows a lineout of the experimental data for the three-pulse case averaged over the transverse direction. The calculation is normalized to the experimental data. The calculation predicts the peak laser emission to occur 150 μm from the surface, which is much further from the surface than the peak gain. While the shape of the experimental data is wider and has a longer tail, there is good qualitative agreement with the position of peak gain. Refraction of the laser has a tremendous impact on the effective gain of the 196-Å line. To estimate the effective gain during the third pulse we varied the target length in the propagation calculation. The resulting amplification from comparing targets of lengths 1.89 and 2.52 cm implies a gain coefficient of 8 cm^{-1}, which is much lower than the peak gain of 30 cm^{-1} shown in Fig. 2 and much closer to the typical gain of 4 cm^{-1}, which has been measured experimentally [7].

In conclusion, we present high-resolution, two-dimensional, spatial images of the 196-Å neonlike germanium laser emission at the output aperture of the laser for targets illuminated by a series of 100-ps pulses from the

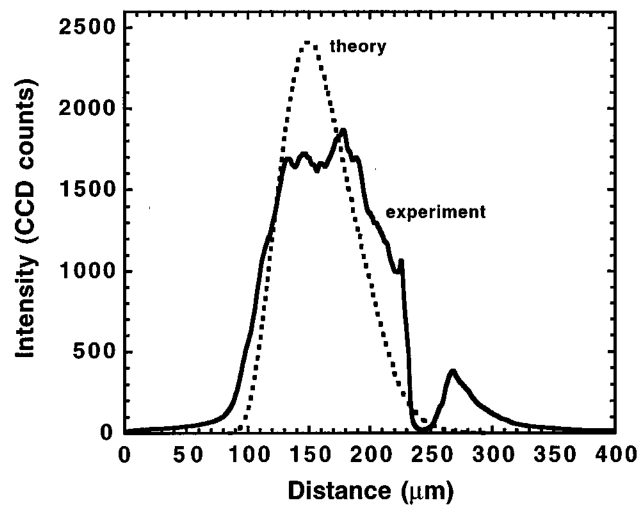

FIG. 4. Spatial dependence of the calculated 196-Å laser intensity (dotted line) at the output aperture of the laser vs distance from the target surface. This is compared with the experimental data (solid line) from Fig. 1, for the case of three pulses, which is averaged over the transverse line focus direction. The uniform background is subtracted from the experimental data.

Nova laser. The images show the peak of the laser emission to occur about 150 μm from the target surface. The simulations show the gain peaking only 50 to 60 μm from the surface, however, our laser transport calculations, which include the refraction effects, predict the peak emission 150 μm from the surface, in good agreement with the experiments. The images do show much structure in both spatial dimensions, which points out the complexity of these plasmas. More imaging experiments are needed to measure the density and gradients in the plasma and to map out the gain profile without the refractive effects to better compare with the simulations.

The authors would like to thank H. Louis, A. Demiris, S. S. Alvarez, and the Nova facilities crew for providing support for the experiments. The support of D. W. Patterson, S. B. Libby, and D. L. Matthews is greatly appreciated. Work was performed under the auspices of the U.S. Department of Energy by the Lawrence Livermore National Laboratory under Contract No. W-7405-ENG-48.

[1] J. Nilsen, B. J. MacGowan, L. B. Da Silva, and J. C. Moreno, Phys. Rev. A **48**, 4682 (1993).
[2] E. E. Fill, Y. L. Li, D. Schlögl, J. Steingruber, and J. Nilsen, Opt. Lett. **20**, 374 (1995).
[3] P. B. Holden and B. Rus, Opt. Commun. **119**, 424 (1995).
[4] J. Zhang, S. T. Chunyu, Y. L. You, Q. R. Zhang, S. J. Yang, W. Z. Huang, D. Y. Wu, X. Q. Zhuang, S. P. Liu, Y. Q. Cai, F. Y. Du, X. D. Yuan, X. F. Wei, Y. K. Zhao, H. S. Peng, and J. Nilsen, Phys. Rev. A **53**, 3640 (1996).
[5] G. F. Cairns, C. L. S. Lewis, M. J. Lamb, A. G. MacPhee, D. Neely, P. Norreys, M. H. Key, S. B. Healy, P. B. Holden, G. J. Pert, J. A. Plowes, C. J. Tallents, and A. Demir, Opt. Commun. **123**, 777 (1996).
[6] A. R. Präg, A. Glinz, J. E. Balmer, Y. L. Li, and E. E. Fill, Appl. Phys. B **63**, 113 (1996).
[7] J. C. Moreno, J. Nilsen, and L. B. Da Silva, Opt. Commun. **110**, 585 (1994).
[8] J. Nilsen and J. C. Moreno, Phys. Rev. Lett. **74**, 3376 (1995).
[9] H. Daido, R. Kodama, K. Murai, G. Yuan, M. Takagi, Y. Kato, I. Choi, and C. Nam, Opt. Lett. **20**, 61 (1995).
[10] A. V. Vinogradov, I. I. Sobel'man, and E. A. Yukov, Sov. J. Quantum Electron. **7**, 32 (1977).

[11] G. Yuan, K. Murai, H. Daido, R. Kodama, and Y. Kato, Phys. Rev. A **52**, 4861 (1995).

[12] J. C. Moreno, J. Nilsen, Y. L. Li, P. X. Lu, and E. E. Fill, Opt. Lett. **21**, 866 (1996).

[13] G. B. Zimmerman and W. L. Kruer, Comm. Plasma Phys. Controlled Fusion **11**, 51 (1975).

[14] J. Nilsen, in *Radiative-Hydro Modeling and Atomic Data Bases*, edited by Allan Hauer and A. L. Merts, AIP Conf. Proc. No. 168 (American Institute of Physics, New York, 1988), pp. 51–58.